Journal of Alloys and Compounds 502 (2010) 225–230

Contents lists available at ScienceDirect

Journal of Alloys and Compounds

journal homepage: www.elsevier.com/locate/jallcom

Fabrication of Nd:YAG transparent ceramics with TEOS, MgO and compound additives as sintering aids

Yukun Li[a,b], Shengming Zhou[a,*], Hui Lin[a,b], Xiaorui Hou[a,b], Wenjie Li[a,b], Hao Teng[a,b], Tingting Jia[a,b]

[a] *Key Laboratory of Materials for High Power Laser, Shanghai Institute of Optics and Fine Mechanics, Chinese Academy of Sciences, Shanghai 201800, PR China*
[b] *Graduate School of Chinese Academy of Sciences, Beijing 100039, PR China*

ARTICLE INFO

Article history:
Received 29 December 2009
Received in revised form 8 April 2010
Accepted 22 April 2010
Available online 4 May 2010

Keywords:
Nd:YAG
Transparent ceramics
Compound additives
Microstructure
Densification

ABSTRACT

1 at.% Nd:YAG transparent ceramics were fabricated by solid-state reaction and vacuum sintering method using commercial Al_2O_3, Y_2O_3 and Nd_2O_3 as raw materials, TEOS, MgO and TEOS combined with MgO were used as additives. When using TEOS or MgO as sintering aids separately, the optimum dosage is 0.5 and 0.2 wt%, respectively. But residual second phases in the grain boundaries and pores are easily generated by adding excessive TEOS or MgO. The maximum transmittance at 1064 nm of the sintered Nd:YAG ceramics is doped 0.4 wt% TEOS combined with 0.08 wt% MgO, nearly pore-free microstructure with the average grain size of more than 30 μm was obtained in this highest transparent sample. All samples sinter to near full density (>99.8%) at 1700 °C and the sample with 0.4 wt% TEOS combined with 0.08 wt% MgO has the highest densification rate. The excellent feature of using compound additives is to make the intensified liquid sintering start at a lower temperature in vacuum sintering, promoting the densification rate and obtaining the uncontaminated crystalline grains.

© 2010 Elsevier B.V. All rights reserved.

1. Introduction

The neodymium-doped yttrium aluminum garnet (YAG) single crystal is the most widely used laser host materials nowadays [1]. But Nd^{3+}concentration is limited under 1.4 at.% as a result of the segregation distribution coefficient (about 0.18 in YAG crystal lattice), bringing about the difficulty in symmetrical homogeneities and highly doping by conventional Czochralski method, thus only part of the fabricated monocrystals is available for the laser application [2]. In order to overcome shortcomings of monocrystals and meet requirements of novel high power solid-state lasers, Nd:YAG transparent ceramics have been rapidly developed since 1984 [3,4]. Ikesue et al. first demonstrated the possibility of obtaining laser output from Nd:YAG transparent ceramics with reasonable efficiency [3,4]. After that, with the development of powder preparing, shaping and vacuum sintering technology, the optical quality of transparent polycrystalline Nd:YAG is equivalent or even better than monocrystal Nd:YAG reported by a lot of studies [5,6].

Many previous studies [7–10] have explained the beneficial role and function mechanism of SiO_2 (usually from the pyrolysis of TEOS) as sintering aid. The beneficial role of silica in sintering kinetics, which was linked to the solid solution formation by substitution of Al^{3+} by Si^{4+} [11], has been reported for many times by an increase of the grain-boundary diffusion coefficient and the decrease of grain-boundary surface energy in the presence of secondary phases [8,10]. Simultaneously, the negative influence of the lattice expansion caused by Nd^{3+}, which has a larger ionic radius (0.112 nm) than the replaced Y^{3+}(0.102 nm), will be effectively eliminated by introducing the Si^{4+}, of which the ionic radius (0.04 nm) is smaller than the replaced Al^{3+}(0.054 nm). Meanwhile the positive effect of adding MgO has also been studied [10,12]. MgO acts as sintering aid and not only substitute Al^{3+} to form $(V_o)^{\bullet}$ [13,8], but also segregate at the grain boundaries to impede the continuous grain growth at the final stage of vacuum sintering [12]. Though the advantageous effects of SiO_2 and MgO in sintering process have been proved definitely, no information has been reported so far on using both TEOS and MgO together as the additives, of which the effect and action mechanism are also unknown yet.

In the resent work, 1 at.% Nd:YAG polycrystalline ceramics were obtained by solid-state reaction and vacuum sintering method, different quantity of TEOS alone, MgO alone as well as TEOS combined with MgO were used as sintering aids. The optimum dosages of the series of additives were provided and the through what action mechanism the additives are efficient, especially the compound additives, was analyzed.

2. Experimental

The commercial high-purity Y_2O_3 (Changchun Haipurui Chemical Co. Ltd., 99.999%), Al_2O_3 (Dalian Rall Fine Ceramic Co. Ltd., 99.99%) and Nd_2O_3 (Changchun Haipurui chenmical Co. Ltd., 99.9999%) powders were mixed according to the stoichiometric $Y_{2.97}Nd_{0.03}Al_5O_{12}$ with different additives and ball milled in alcohol for

---

* Corresponding author. Tel.: +86 021 69918482; fax: +86 021 69918607.
E-mail addresses: heavenliyukun@163.com (Y. Li), zhousm@siom.ac.cn (S. Zhou).

0925-8388/$ – see front matter © 2010 Elsevier B.V. All rights reserved.
doi:10.1016/j.jallcom.2010.04.151

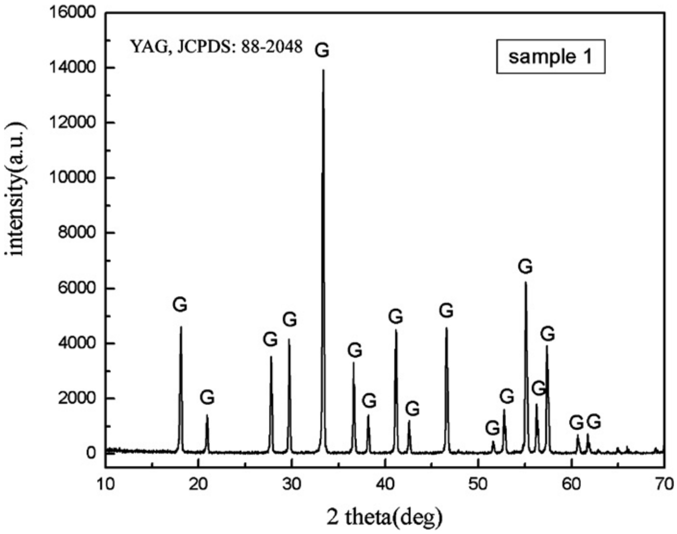

Fig. 1. XRD patterns of Nd:YAG polycrystalline ceramics sample 1, the phase identified is: G(YAG, $Y_3Al_5O_{12}$).

24 h. Then the mixture of powders was dried at 110 °C for 20 h and sieved through 200-mesh stainless steel screen. After that, the powders were pressed with 10 MPa pressure into disks and cold isostatic pressing consolidated at 300 MPa for 5 min. Pre-sintering of the green body was conducted at 1100 °C under air to remove organic wastes. Subsequently, the Nd:YAG polycrystalline ceramics were obtained through sintering under vacuum (1×10^{-3} Pa) at 1750 °C with the soaking time of 20 h. Eventually, the specimens were annealed at 1450 °C for 10 h in air and mirror polished on both surfaces.

The phase structures of the obtained Nd:YAG ceramic samples were indexed by X-ray diffraction (XRD) using a ultima-IV apparatus (Rigaku, Japan). The surface morphologies of the samples were by a JSM6360LA scanning electron microscope (JEOL, Japan) and the elemental compositions were analyzed by EDX attached to the SEM. The optical transmittance spectra including light scattering and absorption spectra were measured with a V-570 UV IS/NIR spectrophotometer (JASCO, Japan). The relative densities were measured by the Archimedes method.

3. Results and discussion

Table 1 shows the samples with the TEOS or MgO alone as additives and Fig. 1 shows the XRD patterns of sample 1. It is seen that the peaks of sample 1 can be well indexed as the cubic garnet structure of YAG (YAG, JCPDS: 88-2048) and the same results were obtained in all the other samples. It indicates that, based on preliminary estimate, full transformation to YAG occurred during vacuum sintering despite the introduction of neodymium and additives.

Fig. 2 shows the optical transmittance spectra of the samples with different quantity of TEOS, all the samples are 1.4 mm thick. The transmittance of the samples in this group increases with the increasing TEOS except sample 5 and the optimum amount of TEOS is 0.5 wt%, which is in consistent with other literatures [14–17].

Table 1
Samples with TEOS or MgO alone.

Sample number	Additive types and content
Sample 1	No addtive
Sample 2	0.3 wt% TEOS
Sample 3	0.4 wt% TEOS
Sample 4	0.5 wt% TEOS
Sample 5	0.6 wt% TEOS
Sample 6	0.1 wt% MgO
sample 7	0.2 wt% MgO
Sample 8	0.3 wt% MgO

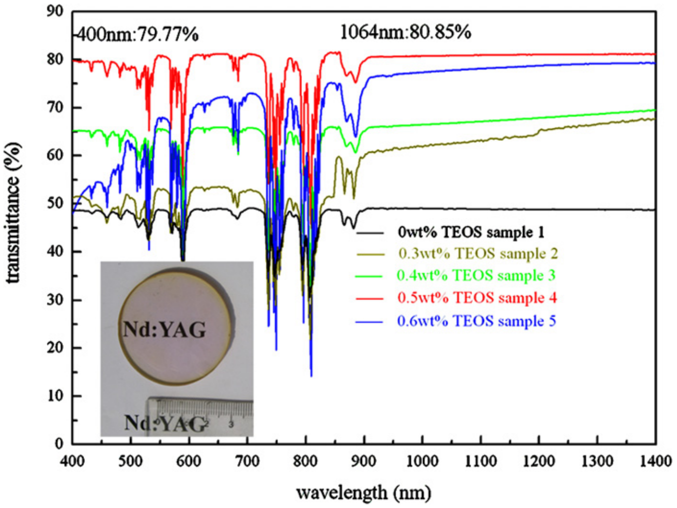

Fig. 2. Optical transmittance spectra (400–1500 nm) of Nd:YAG polycrystalline ceramics sample 1, sample 2, sample 3, sample 4 and sample 5.

The transmittance of sample 4 reaches 80.80% at the wavelength of 1064 nm, and meanwhile a dense and pore-free microstructure is observed in Fig. 3(b), but there are still a few second phases segregated in the grains, the grain boundaries are clean and the average grain size is about 5 μm. The transmittance of sample 5 at 1064 nm is only a little lower compared to sample 4 but decreasing sharply as the wavelength shifts toward the UV range, going down to only 47.95% at 400 nm. Due to the no additive for sample 1, the abnormal grain growth happened as confirmed by the observation of heterogeneous microstructures and the large diameter of the grains as shown in Fig. 3(a). According to the literatures [16,18], a liquid phase which means the beginning of intensified liquid sintering, will be formed from the direct reaction between SiO_2 and YAG round 1380 °C. As seen in Fig. 4 in YAG–SiO_2 phase diagram given by O. Fabrichnaya [19], if only introducing a trace amount of SiO_2, the more SiO_2 is, the more liquid will be formed. The proper liquid is beneficial to the intensified liquid sintering, whereas the overmuch

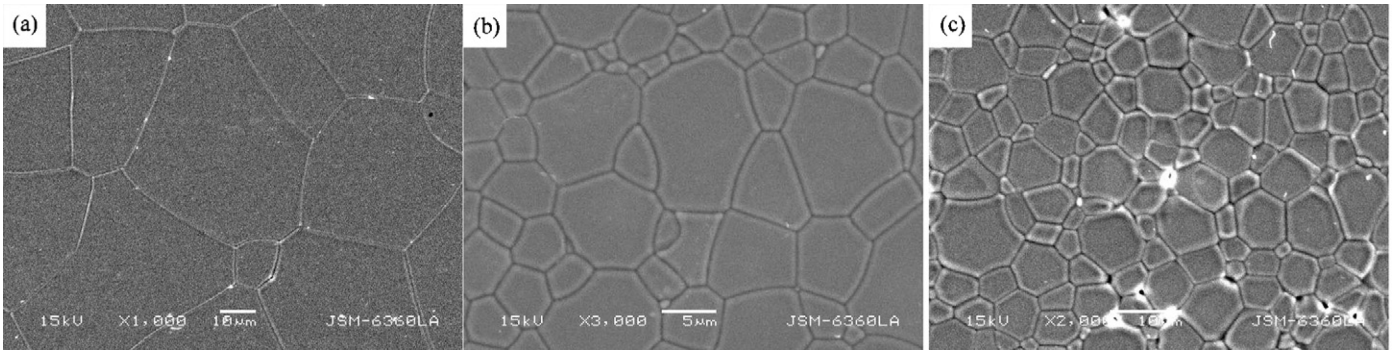

Fig. 3. Surface morphologies of thermal-etched Nd:YAG polycrystalline ceramic sample 1: (a), sample 4: (b) and sample 5: (c).

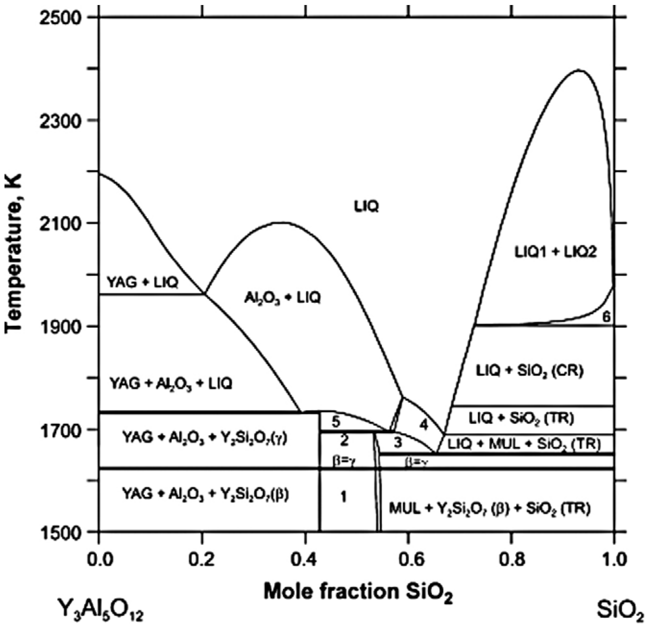

Fig. 4. YAG–SiO_2 phase diagram [19].

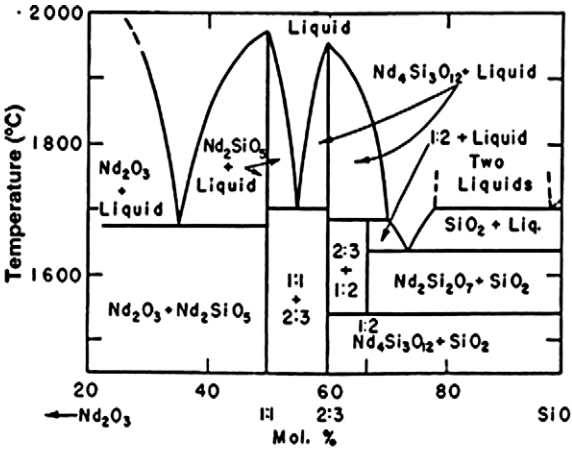

Fig. 5. Nd_2O_3–SiO_2 phase diagram [20].

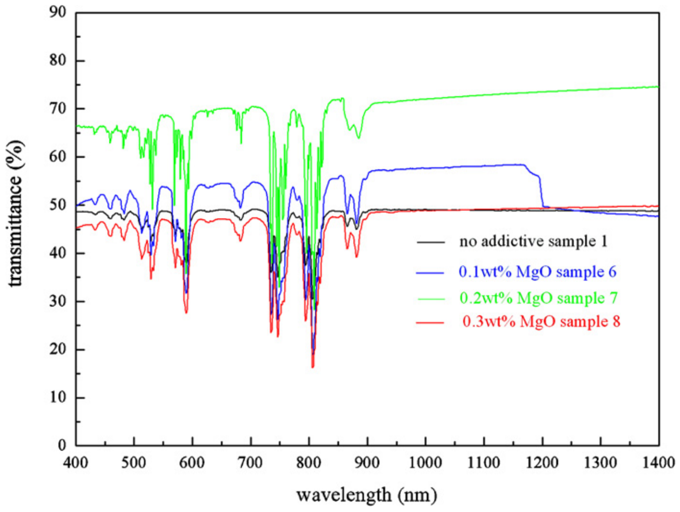

Fig. 6. Optical transmittance spectra (400–1500 nm) of Nd:YAG polycrystalline ceramics sample 1, sample 6, sample 7 and sample 8.

liquid has an opposite effect. As seen in Fig. 3(c), the excessive SiO_2 will lead to residual second phases caused by the grain-boundary segregation, especially at the triple points. Furthermore, while the mass ratio of TEOS changes from 0.5 to 0.6%, according to the molecular weight, the mole ratio of SiO_2 to Nd_2O_3 changes from about 1 to 1.2. The augmentative SiO_2 will increase the amount of the present liquid phase as seen in Fig. 5 in the Nd_2O_3–SiO_2 systems given by Miller and Rase [20]. This is also a probable reason that sample 5 has a worse transparency than sample 4, because the excessive liquid is hard to evaporate totally, finally becoming the scattering particles as the residue. Consequently, the obvious decreasing transmittance toward the UV range for sample 5 is contributed to the intake of excessive TEOS and the variation tendency can be explained according to Mie scattering theory [21].

The optical transmittance spectra of Nd:YAG ceramics for the different concentration of MgO are illustrated in Fig. 6, all the samples are 1.4 mm thick. At normal temperatures, it is more difficult for the solid-state MgO to disperse uniformly in YAG than the liquidus TEOS, but the improving of transparency is obvious as long as the mass fraction of the introducing MgO under 0.2%. In theory, Mg^{2+} will dissolve into Al_2O_3 to replace Al^{3+}, forming the $(V_o)^\bullet$ and boosting the grain-boundary diffusion coefficient [12]. Moreover, MgO will react with YAG to form liquid phase that leads to intensified liquid phase sintering, but at the higher temperature compared to TEOS [12]. It is clearly seen in Fig. 7 that MgO is a useful additive at controlling grain growth and that means, with the increasing MgO the grain sizes of the sintered samples show a distinct decreasing trend. While the dosage of MgO reaches 0.3 wt%, apparent pores, even closed pores will be abundantly formed as shown in Fig. 7(c). The porosity has a dramatic negative impact on light transmission because of the refractive index difference between pores and the surrounding ceramic matrix [22], so the amount of MgO should be carefully controlled.

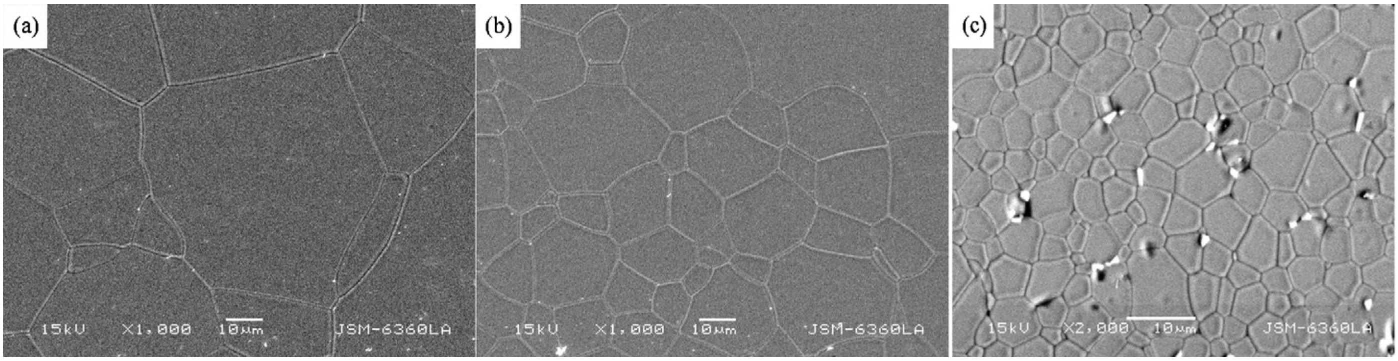

Fig. 7. Surface morphologies of thermal-etched Nd:YAG polycrystalline ceramic sample 6: (a), sample 7: (b) and sample 8: (c).

Table 2
Samples with compound additives.

Sample number	Additive types and content
Sample 9	0.4 wt% TEOS + 0.1 wt% MgO
Sample 10	0.5 wt% TEOS + 0.1 wt% MgO
Sample 11	0.5 wt% TEOS + 0.2 wt% MgO
Sample 12	0.3 wt% TEOS + 0.2 wt% MgO
Sample 13	0.4 wt% TEOS + 0.08 wt% MgO

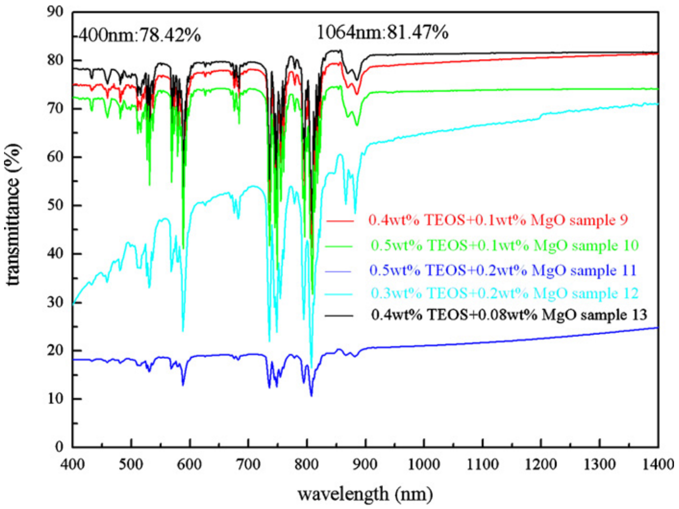

Fig. 8. Optical transmittance spectra (400–1500 nm) of Nd:YAG polycrystalline ceramics sample 9, sample 10, sample 11, sample 12 and sample 13.

Table 2 shows the samples with compound additives, of which the optical transmittance spectra are demonstrated in Fig. 8, all the samples are 1.4 mm thick. It is seen that the transmittance of sample 11 and 12 is very low whatever the wavelength. By contrast, sample 13 owns the best transparency of all. Fig. 9 shows the EDX analysis of sample 4 and 13, the denoted points include the YAG matrix and the segregated second phases. The element composition of Si and Mg are given in Table 3 (0.5 wt% TEOS is equal to 0.14 wt% SiO_2 calculated by the molecular weight). In the zone denoted 1(a) the mass fraction of SiO_2 is 0.46%, which is much higher than the contrivable concentration. It could be explained considering the progressive dissolution of the residual silica into the previous eutectic liquid phase while heat treatment is maintained [18]. And in the YAG matrix denoted 1(b), there is still a small amount of silica, which should disappear above 1700 °C but still exist in the grains. EDX analyze in the zone denoted 2(b) reveals the inexistence of other elements except the YAG matrix. It is supposed that the compound additive is beneficial to obtain the “clean” grains during sintering.

It is interesting to notice in Fig. 8 that the transparency of the sample with 0.4 wt% TEOS combined with 0.1 wt% MgO is better than that with 0.4 wt% TEOS or 0.1 wt% MgO separately. It is deduced that there would be another mechanism in sintering while using compound additives. As shown in Fig. 10 in $MgSiO_3$ system given by Boyd [24], at the condition of very low pressure, a liquid phase appears at the temperature of lower than 1380 °C. Considering the nano-sized starting materials and their high specific surface areas, the SiO_2–MgO liquid would be formed even at a lower temperature, this low-melt-point compound will lead to a higher densification rate. As compared with the YAG formation, the SiO_2–YAG reaction and the MgO–YAG reaction, the reaction between MgO and SiO_2 is posterior to the former but prior to the latter two and that means, the eutectic composition in Y_2O_3–Al_2O_3–SiO_2 or in Y_2O_3–Al_2O_3–MgO system will be replaced by the low-melt-point composition in MgO–SiO_2 system, which also can activate the densification as the fusible silica-based phase or the magnesia-based phase during sintering but disappear at a lower temperature. This characteristic of compound additives is advantageous to transparency boosting. As seen in Table 2, when the dosage of MgO was adjusted from 0.1 to 0.08 wt% as well as keeping the dosage of TEOS 0.4 wt% to make the mole ratio of SiO_2 to MgO more approximately matches $MgSiO_3$, the result in Fig. 8 shows the transmittance of this designed sample reaches as high as 81.47% at 1064 nm, even a little higher than sample 4.

Table 3
Element abundance of Si and Mg in the zone denoted in Fig. 12.

Zone (seen in Fig. 12)	Elements abundance (mass%)	
	Si (SiO_2)	Mg (MgO)
1(a)	0.22 (0.46)	0
1(b)	0.04 (0.10)	0
2(a)	0.07 (0.15)	0.05 (0.07)
2(b)	0	0

Fig. 11 shows the relative densities of some representative samples as a function of sintering temperature with the soaking time of 6 h. All the samples except sample 13 are still in the initial stage of sintering before 1400 °C as proved by their relative densities, which are under 70% of the theoretical value at 1400 °C. For sample 1, relative density increases from 55.7 to 93.8% between 1400 and 1600 °C, approaching 99.8% around 1700 °C. By comparing with relative density curves of sample 1, sample 4 and sample 7, the rapid densification process, which is caused by the intensified liquid sintering, is observed in the latter two. What the difference is, sample 4’s starting time of rapid densification process is earlier than sample 7’s probably for the reason that the reaction temperature between SiO_2 and YAG is lower than that between MgO and YAG. In addition, SiO_2 will increase the diffusivity of Nd^{3+}, accelerating the intermediate stage of solid-state sintering [23]. Particularly, sample 13 has the highest densification rate and the lowest rapid densification starting temperature among all samples. This from the side proves that a liquid phase appears at a temperature lower than that of SiO_2–YAG. Maybe the slightly lower transmittance of sample 13 than sample 4 at the visible-light region can be explained by that the chemical composition of the compound additives is not in conformity with the exact stoichiometric ratio of the formed liquid in $MgSiO_3$ system. Consequently, the direct roles of compound additives are to form the liquid formation through SiO_2–MgO but not SiO_2–YAG, MgO–YAG reaction in sintering, lower the liquid formation temperature, let the intensified liquid sintering start earlier and boost the densification rate.

As seen in Fig. 12, sample 13 has very clean boundaries and the second phases tend to have disappeared totally whatever the zone examined. But unlike other samples with high transparency, such as sample 4 and sample 6, the sample 13 has a much larger average grain size of more than 30 μm, the sample is pore free and there is no evidence of abnormal grain growth. In the final stage sintering (above 1700 °C), there is no second phase locating at the boundaries to prevent the grain growth, so abnormal grain growth would potentially happen in this situation, that is also the reason why sample 13 behaved a relatively larger grain size. According to previous papers [25,26], the grain growth to a critical size relative to the pore size is essential to remove the larger pores, if the sintering is carefully and suitably controlled, that grain growth is an important process to remove the final large pores and to achieve a higher transparency. The best transparent sample at 1064 nm reported up to now is with the average grain size of about 50 μm [25]. For sample 13, relatively density approaches nearly 100% around 1600 °C, this open up the possibility to investigate

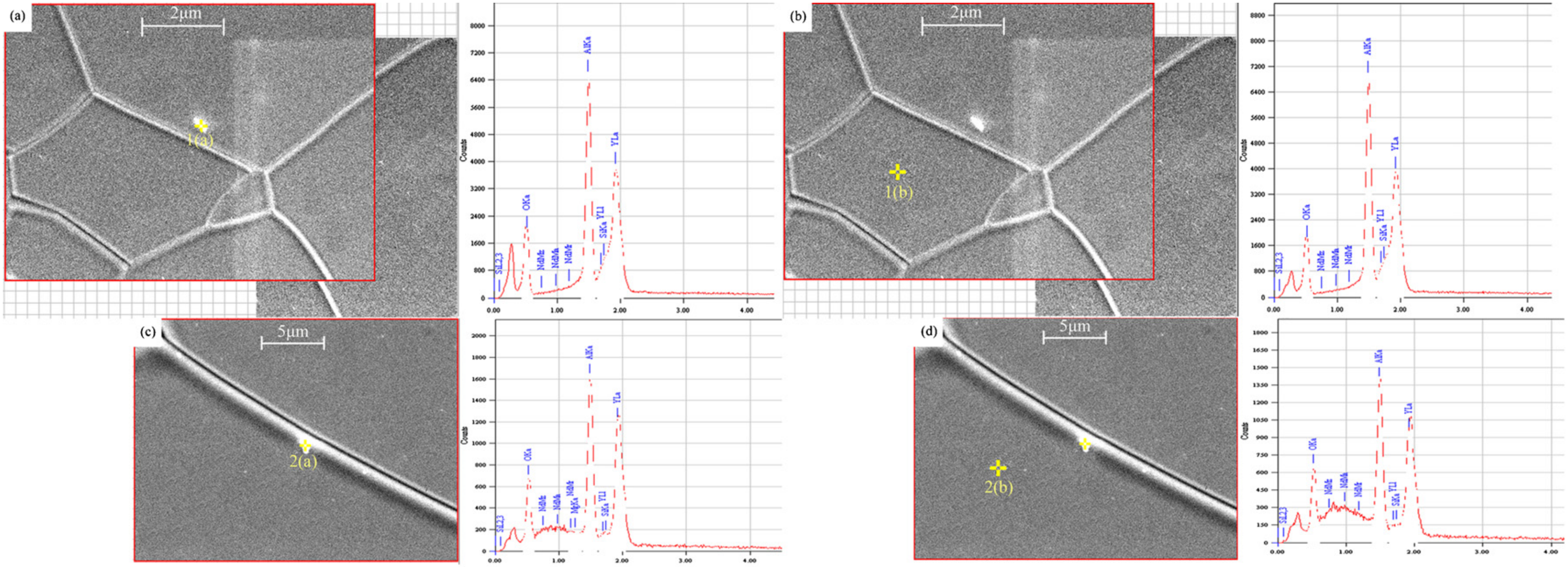

Fig. 9. EDX spectra of denoted zone of sample 4: (a) and (b), and sample 13: (c) and (d).

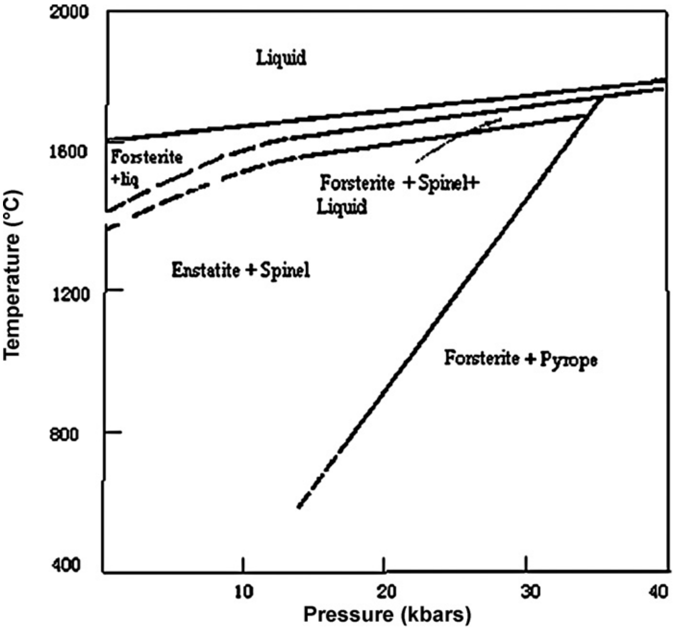

Fig. 10. Temperature–pressure phase diagram of $MgSiO_3$ system [24].

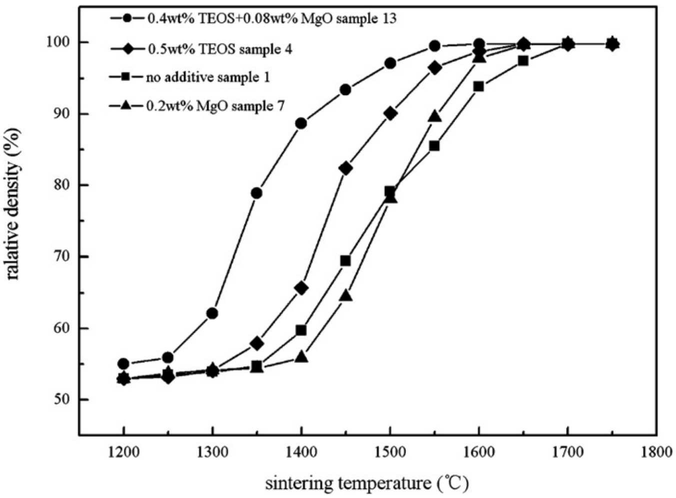

Fig. 11. Relative densities of Nd:YAG ceramics sample 1, sample 4, sample 7 and sample 13 as a function of vacuum sintering temperature.

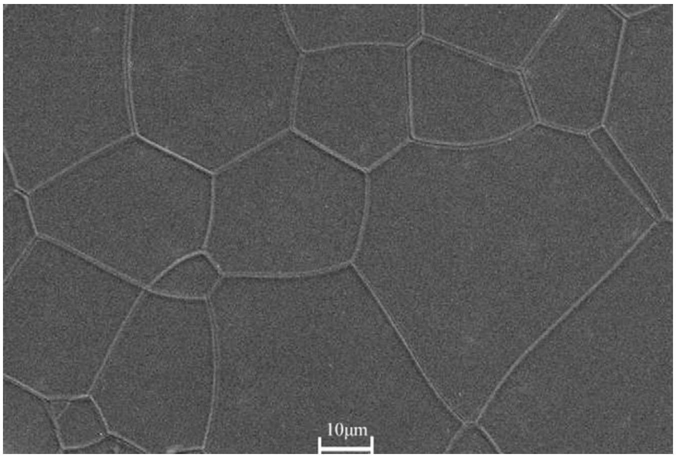

Fig. 12. Surface morphology of thermal-etched Nd:YAG polycrystalline ceramic sample 13.

the low temperature, short-time sintering for samples with compound additives, achieving full density as well as preventing the abnormal grain growth. The aim of future work is to research the “low temperature, short-time” sintering with compound additives and find out in detail the specific action mechanism of compound additives.

4. Conclusion

1 at.% Nd: YAG transparent ceramics were fabricated by solid-state reaction and vacuum sintering method, TEOS, MgO and compound additives (TEOS + MgO) were used as sintering aids respectively. The sample with 0.4 wt% TEOS combined with 0.08 wt% MgO behaved the best transparency at 1064 nm and was possessed of the most densification rate among the all samples. Within a certain range both TEOS and MgO have the positive effect on limiting the abnormal grain growth and promoting transparency, but the excessive TEOS will lead to the residual second phases and the pores are easily formed by adding redundant MgO. The formation and the disappearance temperature of the liquid is a key factor in the vacuum sintering process, the lower liquid formation temperature would lead to the high densification rate and the lower liquid disappearance temperature is beneficial to obtain the large grain size and the uncontaminated grains.

Acknowledgments

The study was supported by the Natural Science Foundation of China (Grant No. 60676004). The authors wish to thank Dr. Xu Xiaodong, for useful suggestions and helpful conversations.

References

[1] N. Daikuzono, Rev. Laser Eng. 21 (1993) 984.
[2] M. Katsurayama, Y. Anzai, A. Sugiyama, M. Koike, Y. Kato, J. Cryst. Growth 229 (2001) 193.
[3] A. Ikesue, I. Furusato, K. Kamata, J. Am. Ceram. Soc. 78 (1995) 225.
[4] A. Ikesue, I. Furusato, K. Kamata, K. Yoshida, J. Am. Ceram. Soc. 78 (1995) 1033.
[5] J.R. Lu, K. Ueda, H. Yagi, T. Yanagitani, T. Akiyama, A.A. Kaminskii, J. Alloys Compd. 341 (2002) 220.
[6] Y. Rabinovitch, D. Tetard, M.D. Faucher, M. Pham-Thi, Opt. Mater. 24 (2003) 345.
[7] G. De With, Philips J. Res. 42 (1987) 119.
[8] A. Ikesue, K. Kamata, J. Ceram. Soc. Jpn. 103 (1995) 489.
[9] G. De With, H.J.A. van Dijk, Mater. Res. Bull. 19 (1984) 1669.
[10] J.W. Vrolijk, G.A. Willems, R. Metselaar, J. Eur. Ceram. Soc 6 (1990) 47.
[11] S.K. Mohapatra, F.A. Kroger, J. Am. Ceram. Soc. 60 (1977) 381.
[12] P.J. Jorgensen, J.H. Westbrook, J. Am. Ceram. Soc. 47 (1964) 332.
[13] A. Ikesue, K. Kamata, K. Yoshita, J. Am. Ceram. Soc. 79 (1996) 1921.
[14] A. Ikesue, Y.L. Aung, Synthesis and performance of advanced ceramic lasers, Conference on Lasers and Electro-Optics/Quantum Electronics and Laser Science Conference, Baltimore, MD, May 2007.
[15] J. Li, Y.S. Wu, Y.B. Pan, W.B. Liu, L.P. Huang, J.K. Guo, Opt. Mater. 31 (2008) 6.
[16] S. Kochawattana, A. Stevenson, S.H. Lee, M. Ramirez, V. Gopalan, D. John, V.K. Castillo, G.J. Quarles, G.L. Messing, J. Eur. Ceram. Soc. 28 (2008) 1527.
[17] S.H. Lee, S. Kochawattana, G.L. Messing, J.Q. Dumm, G. Quarles, V. Castillo, J. Am. Ceram. Soc. 89 (2006) 1945.
[18] A. Maitre, C. Salle, R. Boulesteix, J.F. Baumard, Y. Rabinovitch, J. Am. Ceram. Soc. 91 (2008) 406.
[19] O. Fabrichnaya, H.J. Seifert, R. Weiland, T. Ludwig, F. Aldinger, A. Navrotsky, Z. Metallkd. 92 (2001) 1083.
[20] O. Miller, D.E. Rase, J. Am. Ceram. Soc. 47 (1964) 653.
[21] I. Yamashita, H. Nagayama, K. Tsukuma, J. Am. Ceram. Soc. 91 (2008) 2611.
[22] R. Apetz, M.P.B. van Bruggen, J. Am. Ceram. Soc. 86 (2003) 480.
[23] R. Boulesteix, A. Maitre, J.F. Baumard, Y. Rabinovitch, C. Salle, S. Weber, M. Kilo, J. Eur. Ceram. Soc. 29 (2009) 2517.
[24] F.R. Boyd, J.L. England, B.T.C. Davis, J. Geophys. Res 69 (1964) 2101.
[25] S.-H. Lee, S. Kochawattana, G.L. Messing, J. Am. Ceram. Soc. 89 (2006) 1945.
[26] E.B. Slamovich, F.F. Lange, J. Am. Ceram. Soc. 75 (1992) 2498.